Corrosion inhibition of 6061Al-Si alloy by using Metronidazole in 0.1M HCl Medium

A. S. Fouda[1*], F.I. Al desoky[2], W.T. Elbehairy[1], A.Elmohamad[1]

[1] Department of Chemistry, Faculty of Science, El-Mansoura University, El-Mansoura-35516, Egypt,
[2] Department of Chemistry, Faculty of Science, Port Said University, Egypt
[*]E-mail: asfouda@hotmail.com, asfouda@mans.edu.eg

The corrosion behavior of 6061Al-Si alloy in 0.1M HCl in the being present of Metronidazole(MNZ) compound has been observed using open circuit potential(OPC), AC impedance (EIS), Tafel diagrams, electrochemical frequency modulation (EFM)and weight reduction (WR) methods. The protective efficacy (IE) rises by raising the Metronidazole extent (MNZ) and diminished by raising the temperature. Tafel diagram has shown that the Metronidazole acts as a mixed-kind inhibitor. MNZ adsorption on the alloy surface was obeying Temkin isotherm. The surface analysis of Al alloy was performed by scanning electron microscope (SEM), AFM (atomic force microscopy) and Fourier transform infrared spectra (FT-IR).

Keywords: Corrosion, Adsorption, Al alloy, HCl, SEM, AFM, FTIR

1. INTRODUCTION

Pharmaceutical drugs like heterocyclic compounds are used in the reduced corrosion process of Fe, Cu and Al [1-11] in various aqueous media. Adsorption of the drug facilitates the protection of the metal surface [12]. A few medications such as tetracycline, cloxcillin, azithromycin, ampiclox, ampicillin and orphenadrine were discovered to have a great inhibition for corrosion of metals and alloys. The corrosion inhibitors that contain heteroatoms resembling O, S or N atoms. The IE of inhibitors is depends on the structure and chemical properties of the film present on the metals. The current study reports the performance of metronidazole, the objective of this research is to examine the inhibiting behavior of Metronidazole on the corrosion of Al-Si alloy in 0.1 M HCl utilized chemicals and electrochemical tests. The sample surface analyses were also analyzed. Metronidazole (MNZ) is an antibiotic and antiparasitary drug used for the treatment of abdominal inflammatory disease [13].
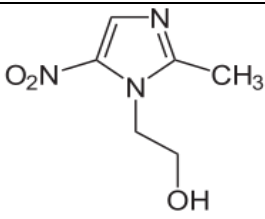
2. MATERIALS AND TECHNIQUES

2.1. Materials and solutions

The metal sample conformation in weight % is: Si 0.67, Fe 0.19,Cu 0.24, Mn < 0.01, Mg 1.00, Cr 0.05,Zn 0.01,Ti 0.02 and Al the rest

2.2. Inhibitor

Table 1describs the Metronidazole (MNZ) structure.

Table 1. Chemical assemblies of the MNZ.

Structure	IUPAC Name	Molecular weight	Active center	Chemical formula
O_2N ... CH_3 ... OH (imidazole structure)	2-(2-methyl-5-nitro-1H-imidazol-1-yl)ethanol	171.15 g/mol	3N 3O 2π bonds	$C_6H_9N_3O_3$

2.3. Chemicals and solutions

Al-Si alloy specimens were used. The aggressive medium used is HCl 37%.Solutions of 0.1 M HCl were prepared by dilution with distilled water. The metronidazole stock solution 10^3 ppm was used to prepare (50,100,150,200,250 and 300 ppm).

2.4. Methods

2.4.1. Mass loss (ML) technique

The coins with size (2 × 2 × 0.2 cm) x2 were dipping in 100 ml of 0.1M HCl and existence of the various contents of MNZ are set in water thermostat. After 3 hrs the samples were removed, rinsed, dried, and weighed again. The % IE and the θ were founded from Eq. (1)

$$\% \text{ IE} = \theta \times 100 = [(W^o − W) / W^o] \times 100 \tag{1}$$

Where W^o and W are the weights of nonexistence and occurrence of MNZ, individually.

2.4.2 Open‑circuit Potential (E_{OC}) Method

The working electrode was immersed in 0.1MHCl (100ml) for 30 min to establish a steady state E_{OCP}.

2.4.3. Potentiodynamic polarization technique

This technique was done in a typical three compartment glass cell.The potential range was (-1.0 to - 0.6V vs. SCE) at OCP with a scan rate 1 mVs^{-1}.

2.4.4. EIS technique

This technique was done by AC signs of 5 mV peak to peak amplitude and at frequency range of 10^7 Hz to 0.1 Hz. The (% IE) and θ were founded from eq. (2) [14]:

$$\% \text{ IE} = 100 \text{ x } \theta = 100 \text{ x } [(R_{ct} - R^{\circ}_{ct})/ R_{ct}] \tag{2}$$

Where, R°_{ct} and R_{ct} are the charge transfer resistances without and with MNZ, individually.

2.4.5- EFM test

This technique used two frequencies of range 2 and 5 Hz depended on three conditions [15]. The (i_{corr}), (β_c and β_a) and (CF-2, CF-3) (Causality factors) were measure by the greater two peaks[16].

2.4.6. Surface examination

Al alloy pieces were dipped in testing solutions for one day. Then, they were polished, dried and analyzed by (SEM), (FTIR) and (AFM).

3. RESULTS AND DISCUSSION
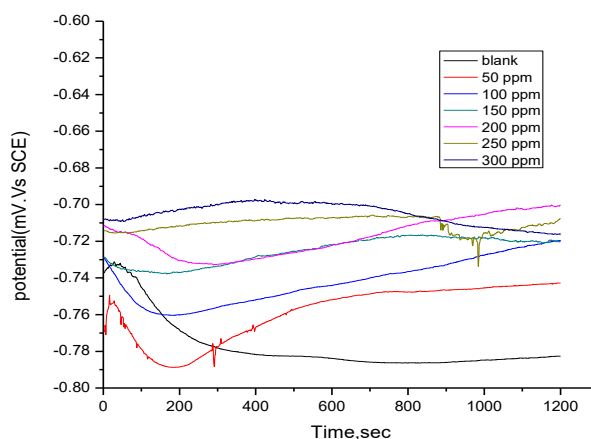
3.1. Open‑circuit Potential (EOC) Method

Figure 1. Open-circuit potential diagram for Al alloy electrode in 0.1 M HCl without and with various concentrations of Metronidazole at 25 °C

The E_{OC} method indicates the changes which take place on alloys and metal surfaces such as oxidation, presence of the protective layer or immunity during the immersion in the corrosive media. Figure 1 shows the E_{OC} curves for 6061Al-Si alloy dipped in 0.1M HCl without and with many contents of Metronidazole at 25 °C. It shows that the E_{OC} is shifting toward more negative potentials resulting from dissolution process. The E_{OC} gradually increases due to the foundation of the shielding film of MNZ on the surface, which confirms the possibility of using the MNZ as a corrosion inhibitor [17].

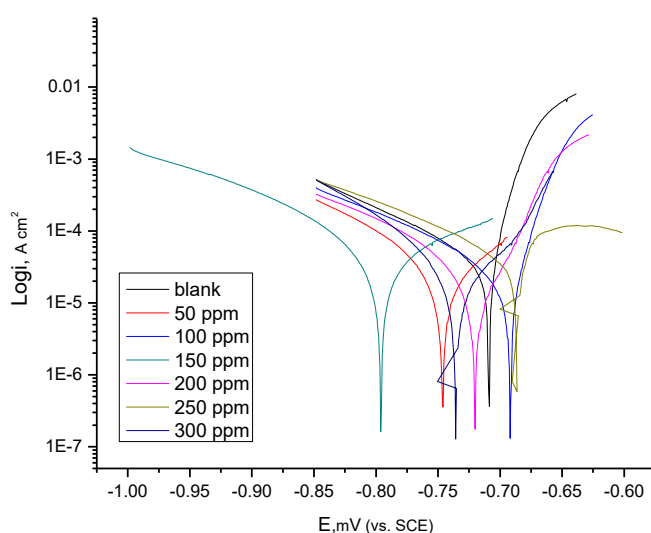*3.2. Potentiodynamic polarization tests*

Figure 2. Polarization curves of the Al alloy dissolution with and without different concentrations of Metronidazole at 25°C

Table 2. Potentiodynamic polarization results of Al alloy dissolution with and without different concentrations of MNZ at 25°C

Conc., ppm	i_{corr}, $\mu A\ cm^{-2}$	$-E_{corr}$, mV vs SCE	β_a mV dec^{-1}	β_c mV dec^{-1}	C.R Mpy	Θ	% IE
0	22.1	709	15.8	79.1	31.6	--------	-------
50	15.6	746	58.0	51.1	22.3	0.294	29.4
100	10.6	692	18.2	56.7	15.2	0.520	52.0
150	10.3	796	31.1	27.8	14.8	0.534	53.4
200	7.7	720	32.1	36.7	11.0	0.652	65.2
250	2.7	736	20.6	29.4	3.8	0.878	87.8
300	2.5	688	11.9	24.1	3.5	0.887	88.7

Tafel curves of Al alloy electrode in 0.1M HCl with and without various contents of Metronidazole can be studied from figure 2. From Table 2 MNZ was affected both the cathodic and

anodic processes and the IE rises with raising the MNZ content. E_{corr} was a little changed, indicating that MNZ acts as a mixed–kind inhibitor. i_{corr} declines clearly with the MNZ addition to 0.1M HCl. % IE and (θ) were found from eq. (3):

$$\% \text{ IE} = \theta \times 100 = [(i_{corr} - i_{corr(inh)}) / i_{corr}] \times 100 \tag{3}$$

Where i_{corr} is the corrosion current without MNZ and i_{corr} with MNZ.

3.3. (EIS) tests

From figure 3 the semi-circle diameter was risen by increasing of MNZ concentration. Figure 4 indicates the utilizing circuit for fitting the obtained results [18]. The C_{dl}, Y^0 and n were founded from eq. (4) [19]:

$$C_{dl} = Y^0 \omega^{n-1} / \sin [n (\pi/2)] \tag{4}$$

where $\omega = 2\pi f_{max}$, f_{max} is the greater frequency and n is the exponential. R_{ct} increases with the rise of the double layer thickness [20]. From table 3, the C_{dl} decline attributable to the replacement of adsorbed water molecules by MNZ species [21].
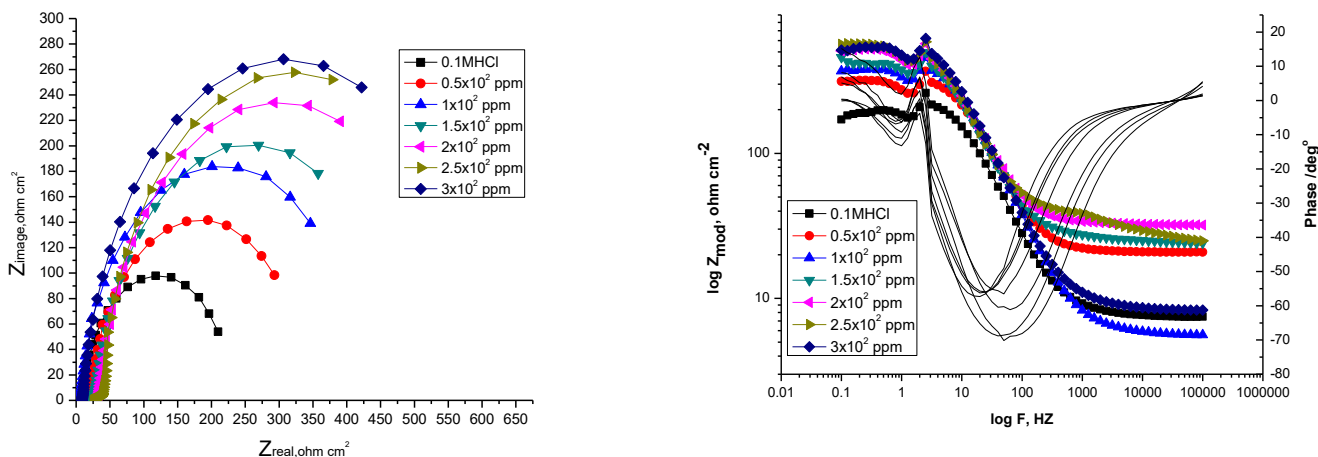

Figure 3. EIS Bode and Nyquist curves for Al-Si alloy in 0.1MHCl using and non-using several contents of Metronidazole 25°C
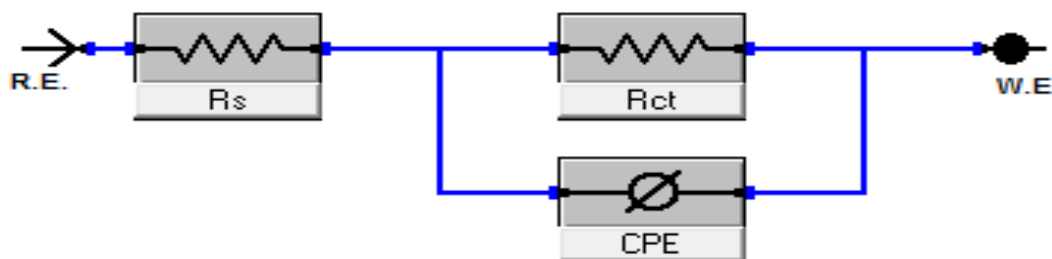

Figure 4. Circuit utilized for fitting the EIS data in 0.1M HCl.

Table3. EIS parameters for the tested alloy without and with different concentrations of MNZ at 25°C

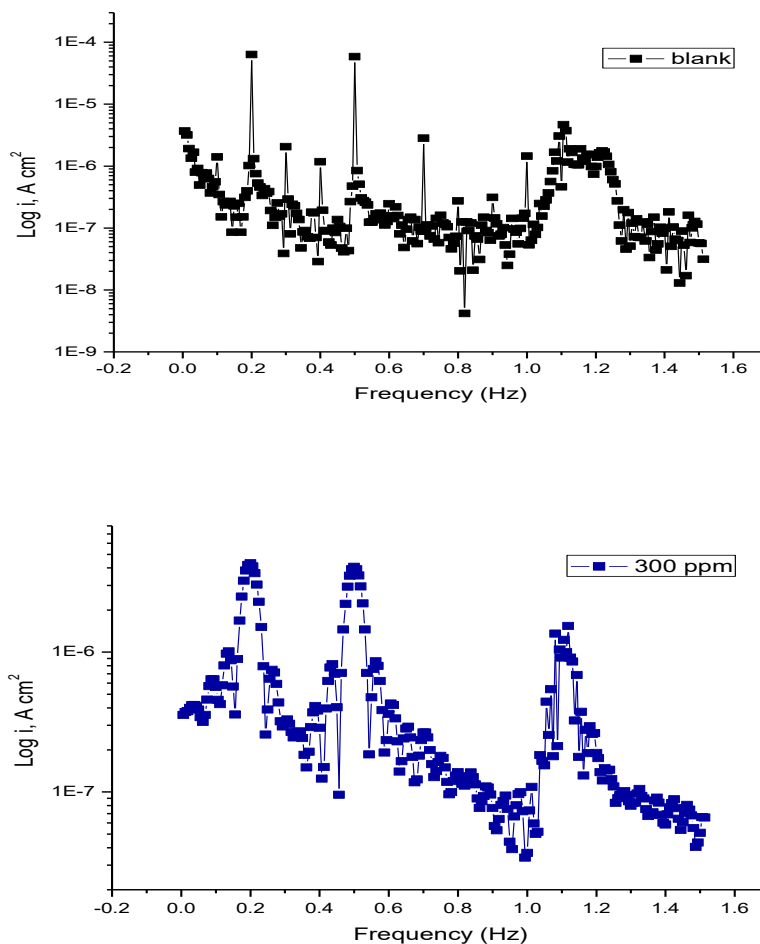| Conc.,ppm	R_{ct}, Ω cm^2	C_{dl}, μFcm^{-2}	θ	% IE
0	142.2	177.1	----	----
50	286.2	60.4	0.503	50.3
100	368.2	58.6	0.614	61.4
150	387.6	57.2	0.633	63.3
200	464.5	53.8	0.694	69.4
250	518.2	51.5	0.726	72.6
300	523.3	26.3	0.728	72.8

3.4. (EFM) tests

Figure 5. EFM diagrams for Al-Si alloy without and using of 300ppm MNZ at 25°C

EFM is a safety dissolution technique which is characterized by speed and accuracy in calculating the current data from Tafel slopes [22]. Figure 5 indicates the EFM of Al-Si alloy in 0.1M HCl solution and 300ppm of MNZ. The EFM parameters such as (CF-2 and CF-3), (β_c and β_a) and (i_{corr}) can be measured from the higher current peaks. The CF is closer to the standard data proved the validity and quality of the calculated data. The IE% increase with the raising of MNZ concentrations.

Table 4. Parameters of EFM diagrams for Al-Si alloy without and with many MNZ concentrations in 0.1M HCl at 25°C

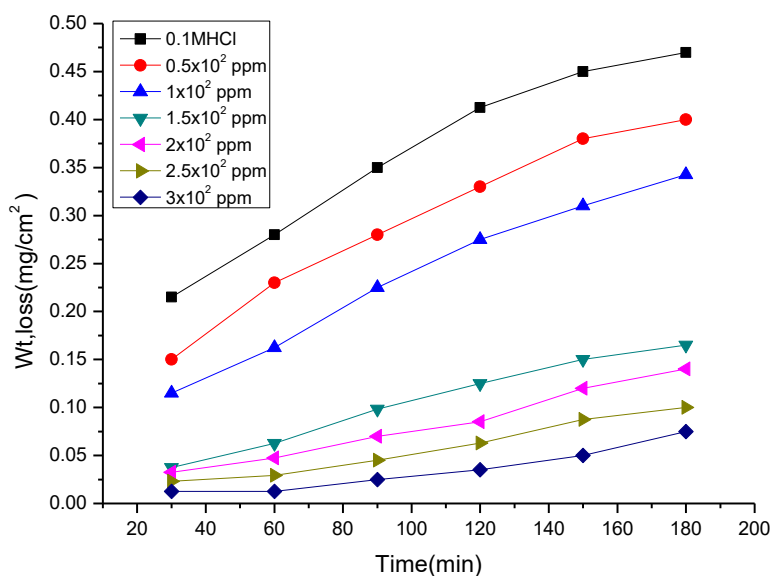| Conc., ppm	i_{corr} µAcm^{-2}	β_c, mVdec^{-1}	β_a, mVdec^{-1}	C.R , mpy	CF-2	CF-3	Θ	%IE
0	99.9	122.9	94.5	142.9	1.9	2.9	-	-
50	85.6	151.6	117.3	122.5	2.1	3.2	0.143	14.3
100	69.8	142.9	120.0	99.8	2.3	2.8	0.301	30.1
150	54.7	164.5	145.6	78.3	1.7	3.4	0.452	45.2
200	49.9	117.2	108.2	65.6	1.9	3.0	0.501	50.1
250	40.2	110.3	102.2	57.4	2.0	2.5	0.598	59.8
300	3.1	54.3	44.1	44.8	1.8	3.2	0.969	96.9

3.5. Mass loss (ML) tests

Figure 6. ML-time curves for the corrosion of Al-Si alloy without and using many Metronidazole concentration at 30°C

Table 5. Values of IE after 120 min of Al-Si alloy without and using many concentration of MNZ at 30ºC

[inh.], Ppm	Metronidazole compound	
	% IE	Θ
50	20.0	0.200
100	48.3	0.483
150	65.7	0.657
200	79.4	0.794
250	87.7	0.877
300	95.5	0.955

The reduction in mass of Al alloy coins non-using and using different MNZ contents at 30°C. Figure 6 shows that MNZ decreases the mass reduction and the corrosion rate. The (%IE) and then θ, of the MNZ for the Al alloy were founded by eq. (1) [23]. The values of %IE are given in Table 5.

3.6. Influence of temperature

The Table 6 indicates that %IE reduces with rising the temperature (Figure 6). The decrease in % IE with the rising the temperature proving the physical adsorption of MNZ.
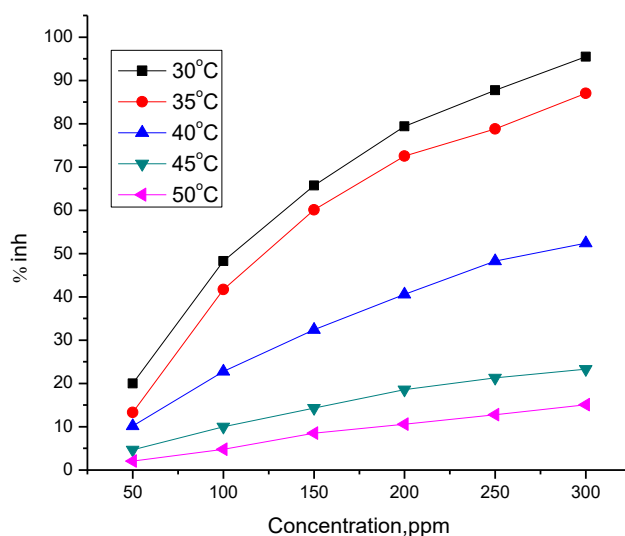

Figure 6. The relationship between % IE and temperature at many Metronidazole concentrations for Al alloy corrosion

Table 6. Parameters such as %IE, (θ) and (C.R.) for Al alloy dissolution after 120 min without and using many Metronidazole concentrations at a range of temperatures

Conc., ppm	Temp, K	C.R., mg cm^{-2} min^{-1}	Θ	%IE
Blank		3.2	------	------
50		2.8	0.200	20.0
100		1.8	0.483	48.3
150		1.2	0.657	65.7
200	303	0.7	0.794	79.4
250		0.4	0.877	87.7
300		0.2	0.955	95.5
Blank		3.4	----	-----
50		2.9	0.133	13.3
100	308	2.0	0.417	41.7
150		1.4	0.601	60.1
200		0.9	0.725	72.5
250		0.7	0.788	78.8
300		0.4	0.870	87.0
Blank		3.5	-----	------
50		3.0	0.102	10.2
100		2.3	0.228	22.8
150	313	2.0	0.324	32.4
200		1.8	0.406	40.6
250		1.6	0.483	48.3
300		1.4	0.524	52.4
Blank		3.6	------	------
50		3.4	0.047	4.7
100		3.2	0.100	10.0
150	318	3.1	0.143	14.3
200		2.9	0.186	18.6
250		2.8	0.213	21.3
300		2.7	0.233	23.3
Blank		3.9	------	------
50		3.8	0.021	2.1
100		3.7	0.048	4.8
150	323	3.6	0.085	8.5
200		3.5	0.106	10.6
250		3.4	0.128	12.8
300		3.3	0.151	15.1

The equation of Arrhenius (6) can be used to measure the activation energy (E^*_a) of the activated complex [24]:

$$C.R. = A \exp (-E^*_a / RT) \tag{5}$$

where E^*_a is activation energy and T is the absolute temperature. The E^*_a was founded from Figure 8 (Table 7). E^*_a values prove that the MNZ impedes corrosion effectively in the presence of higher extents by raising the energy barrier of the activated complex and improve that the process is controlled by diffusion [25]. (ΔH^*, ΔS^*) are founded from eq. (7) [26]:

$$\text{C.R.} = RT/Nh \exp (\Delta S^*/R) \exp (-\Delta H^*/RT) \tag{6}$$

Figure 9 shows the relation between log (C.R. /T) and (1/T) which used to measure the values of ΔH^* and ΔS^* (Table 7).
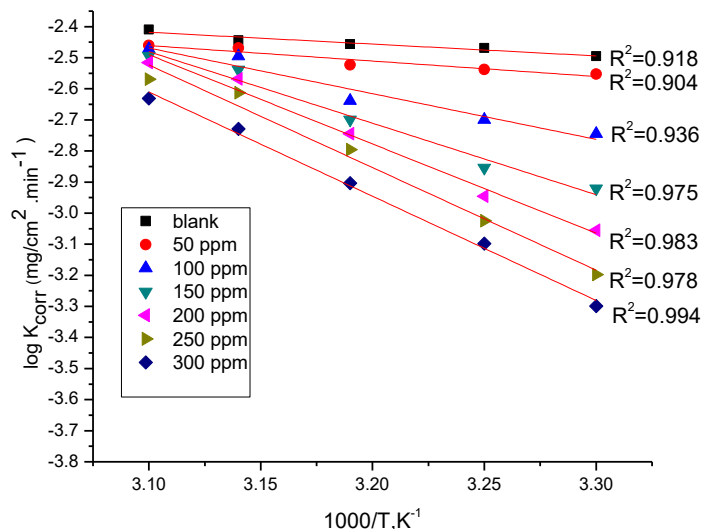

Figure 8. Log k_{corr}. vs reciprocal of temperature plot for Al alloy non-using and using many Metronidazole concentrations

In the chemisorption process, enthalpy must be or more than 100 kJ mol⁻¹[27]. The rise in the (ΔH^*) with the occurrence of the MNZ reflects the rise in the energy barrier of the corrosion procedures. The negative values of ΔS^* show that during the rate-determining step in the formation of activated complex is more frequent than the cracking [28].
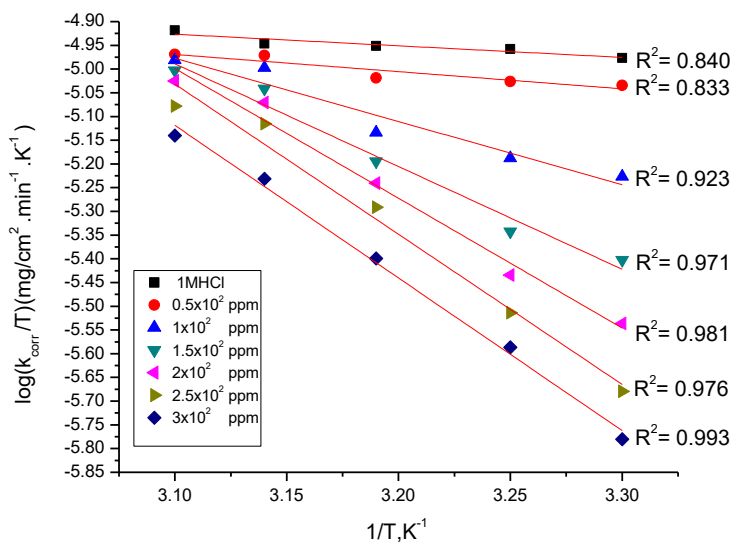

Figure 9. The relation between log C.R. / T) and 1/ T diagrams for the Al alloy without and with several MNZ concentrations

Table 7. Data of activation for Al alloy without and with range of MNZ concentrations

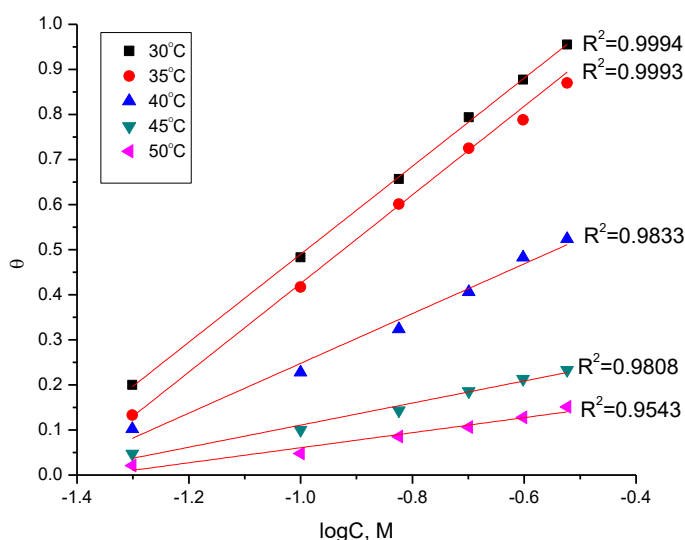| Conc., ppm	E_a^*, kJ mol^{-1}	ΔH^*, kJ mol^{-1}	$-\Delta S^*$, J mol^{-1}K^{-1}
0	7.3	4.7	277.2
50	9.5	6.9	271.1
100	28.1	25.5	213.6
150	44.1	41.4	164.5
200	55.0	52.4	130.9
250	63.2	60.6	106.0
300	64.2	61.6	104.6

3.8. Adsorption isotherms

Figure 10. Temkin isotherm for the MNZ adsorption on Al alloy in 0.1M HCl

Figure 10 represented the Temkin isotherm, which used to calculate Θ values for MNZ. The Temkin equation represented as follows [29].

$$\Theta_{coverage} = (2.303/a)\ Log\ K_{ads} + (2.303/a)\ Log\ C \tag{7}$$

Where K_{ads} is the adsorption constant, C is the MNZ content (M) and "a" (Heterogeneous factor of surface of the metal).

Plotting (Θ) vs (Log C) of MNZ at 30ºC to 50ºC (Figure 10). The ΔG°_{ads} and K_{ads} data are in Table 8. The ΔG^{o}_{ads} founded by:

$$\Delta G^{o}_{ads} = -\ RT\ ln\ (55.5\ K_{ads}) \tag{8}$$

The MNZ adsorption is spontaneous and this is proven by the ΔG°_{ads} negative sign. From the data of ΔG^{o}_{ads} (around to -20 kJ mol^{-1}), proven that the MNZ adsorption is physisorption [30].

Vant't Hoff equation can be used to measure ΔH°_{ads} and ΔS°_{ads} [31] expressed by:

$$\text{Ln K}_{ads} = \frac{-\Delta H^{\circ}_{ads}}{RT} + const \tag{9}$$

And eq. (10):

$$\Delta G^{o}_{ads} = \Delta H^{o}_{ads} - T \Delta S^{o}_{ads} \tag{10}$$

Figure 11 shows the relation between ΔG^{o}_{ads} and T. A negative sign of ΔS^{o}_{ads} proved that the disorder decreasing of corrosion process by using MNZ (Table 8) [32].
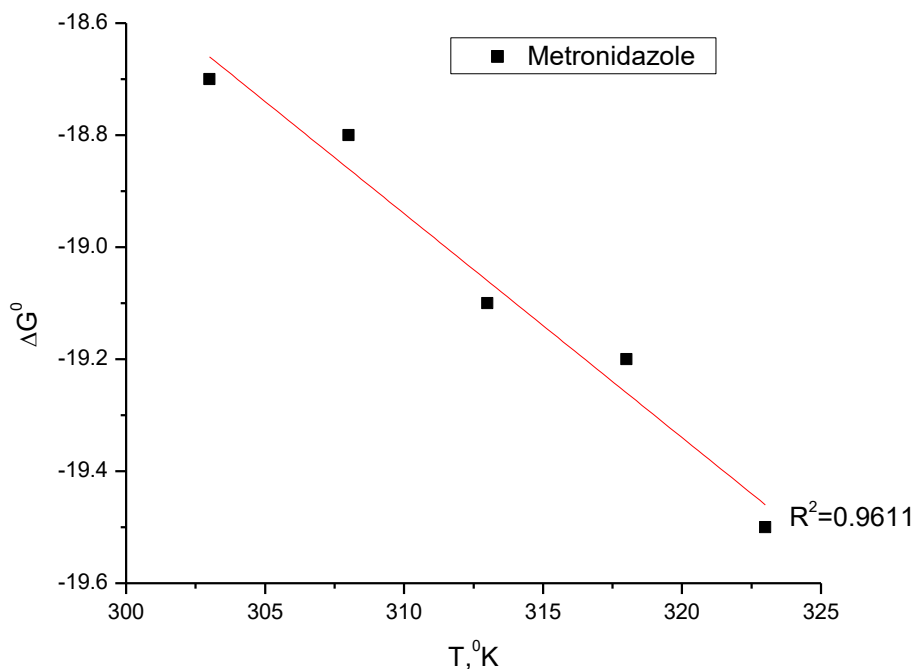

Figure 11. Plots ΔG°_{ads} vs T for the MNZ adsorption in 0.1M HCl

Table 8. Temkin data for Al alloy without and using changed MNZ contents at (30°C- 50°C)

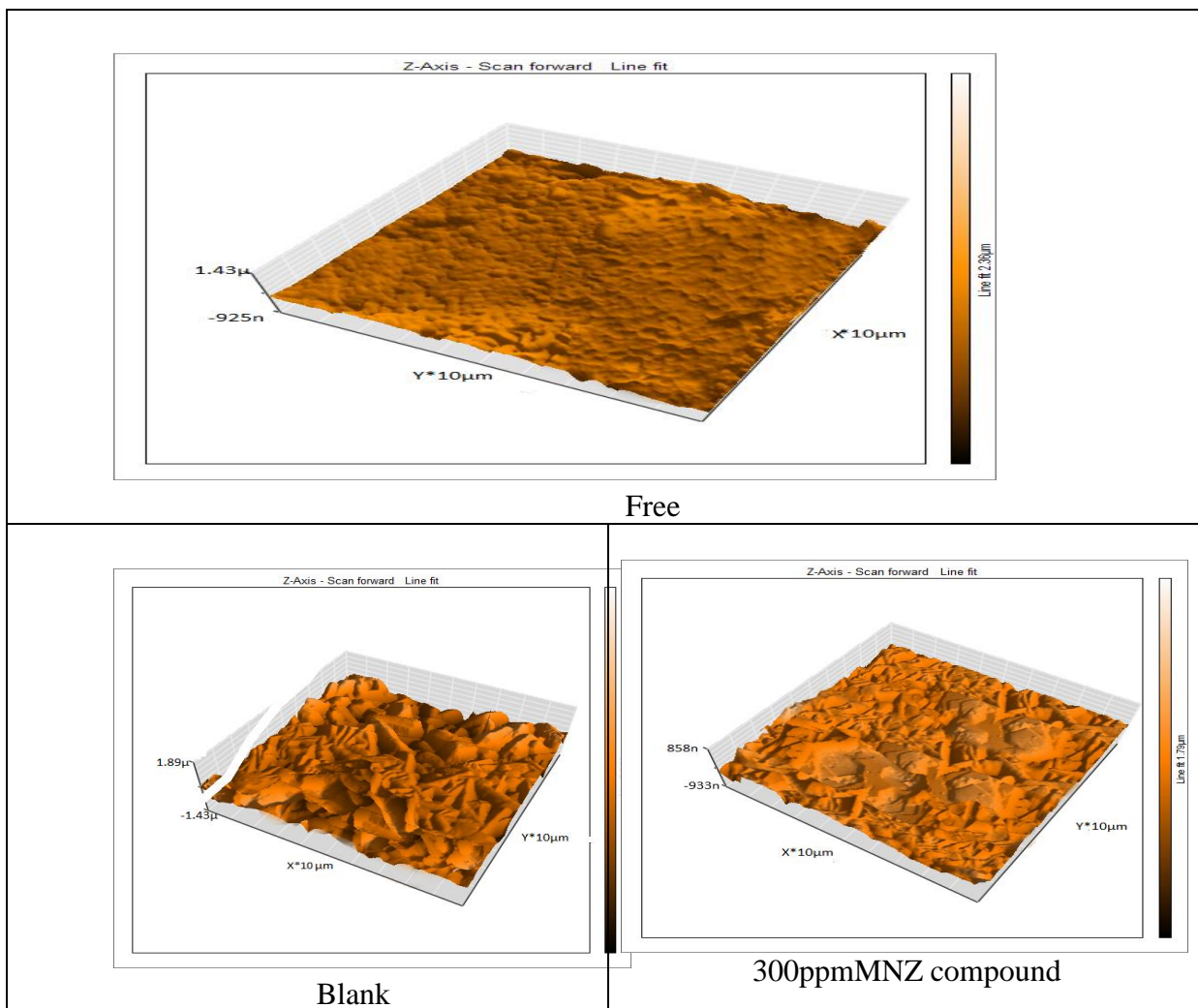| Temp., K	K_{ads} M^{-1}	-ΔG°_{ads} kJ mol^{-1}	-ΔH°_{ads} kJ mol^{-1}	-ΔS°_{ads} J mol^{-}K^{-1}
303	31.8	18.7		40.0
308	28.3	18.8		39.9
313	28.1	19.1	6.5	40.3
318	27.0	19.2		39.9
323	23.1	19.5		40.2

3.9. (AFM) analysis

Figure 12. (3D) AFM images of 6061 Al-Si alloy without acid (free), Al alloy in 0.1M HCl (blank), and Al alloy in 0.1 M HCl at 300 ppm of MNZ for 24 hours at 25^oC

This method gives a map of the metal surface where roughness are indicated with an excessive resolve [33]. The 3D images of AFM shown in Figure 12.

Table 9. AFM parameters for 6061 Al alloy (a) pure coin (b) with for 24 hours   (c) with corrosive medium containing 300 ppm MNZ for 24 hours

Parameters	A	B	C
The roughness average (Sa)	48.6	391.8	94.6
The mean value (Sm)	-16.6	-18.7	-18.1
The root mean square (Sq)	125.0	471.8	143.3
The valley depth (Sv)	-644.5	-1272.8	-794.2
The peak height (Sp)	621.1	1562.2	444.2
The peak-valley height (Sy)	1205.5	2434.9	1232.3

From the table, the surface of the Al alloy is smoothened in the presence of the MNZ resulting from MNZ adsorption therefore the acid attack was reduced[34].

3.10- SEM test

Figure 13, suggests the micrograph given for Al alloy sheets in absence and using 300 ppm of MNZ after dipping for only one day.
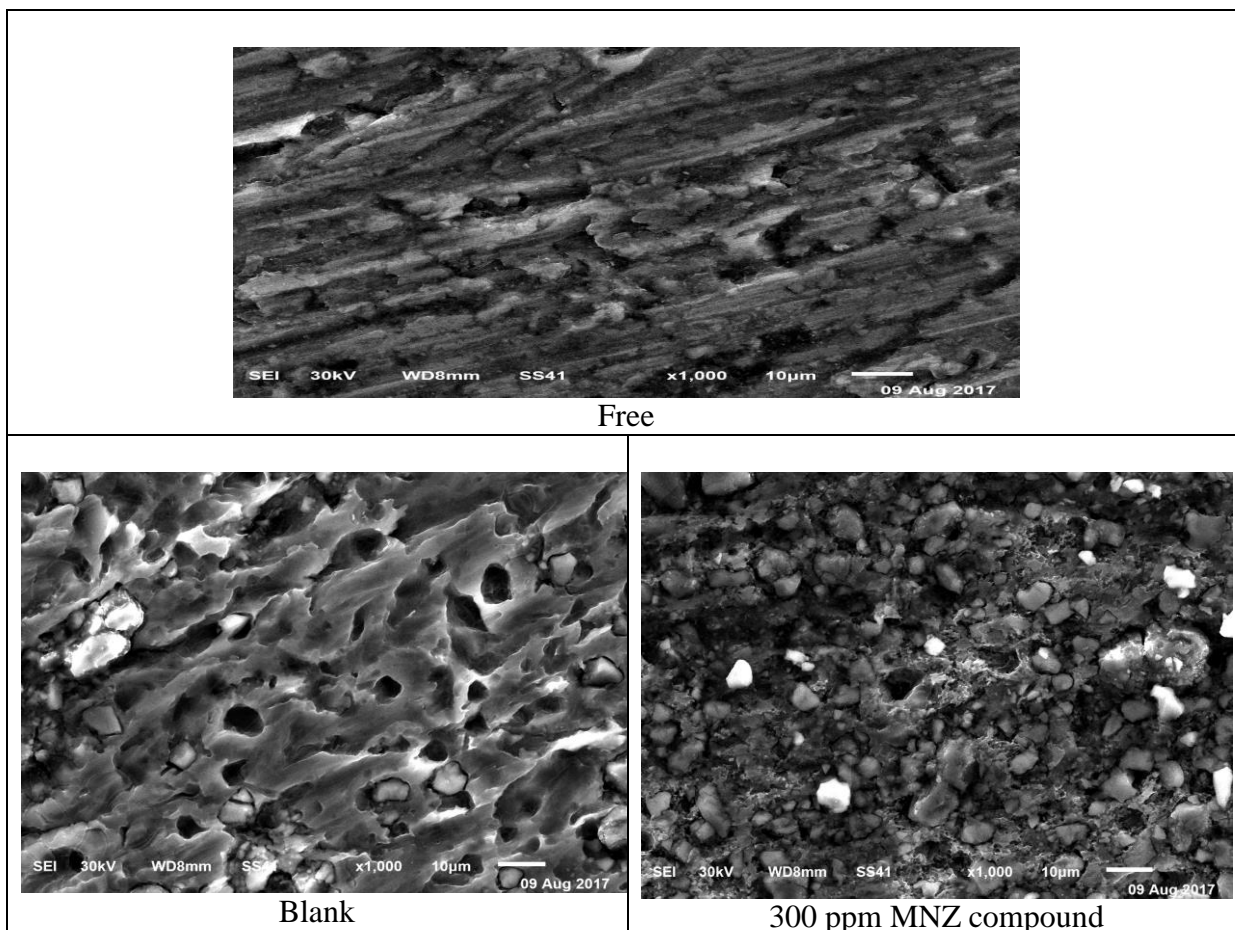

Figure 13. SEM image for Al alloy with and without 300 ppm of study compound after immersion for 24 hours at 25°C

From SEM image, the Al alloy surface is more degradation due to damaging corrosion attack in the blank solution. The MNZ adsorption on the Al alloy surface, creating the shielding layer resulting in blocking the surface active centers so that the surface became more smooth [35].

3.11. MNZ action mechanism

The metronidazole action mechanism as a corrosion inhibitor for Al-Si alloy in 0.1 HCl solution was discussed in terms of adsorption of this molecule physically on the alloy surface. This indicated from the values of ΔG^o_{ads} (less than 20 kJ mol^{-1}) and also from the effect of temperature

(%IE decreases by raising temperature). This molecule (metronidazole) will present in the protonated form, so it can not adsorb on the positive alloy surface. First Cl⁻ ions adsorbed on the alloy surface and after that the MNZ (protonated form) will adsorb on the alloy surface by electrostatic attraction. The following Table (10) gives a comparison of %IE with different investigated drugs. The present drug gives considerably significant corrosion %IE compared to other drugs. Thus, the present MNZ drug can be used as corrosion inhibitor with promising results.

Table 10. Performance comparison of some expired drugs as corrosion inhibitors

Inhibitor(drug)	sample	Medium	IE%	References
Antihypertensive(Enalapril maleate)(0.2M)	6063Al-Si alloy	0.01M HCl	73.4	36
Voltaren (125ppm)	Al	1M HCl	89.7	37
ampicillin (Amp) (1000ppm), cloxacillin (Clox) (1000ppm), flucloxacillin(Fluclox) (1000ppm) amoxycillin(Amox) (1000ppm)	Al	2MHCl	85.5 80.0 77.5 90.0	38
Cefuroxime Axetil(0.5g/L)	Al	0.1MHCl	81.3	39
Theophylline Anhydrous ($5x10^{-4}$M)	Al	2MHCl	99.9	40
Cefadroxil(5) ($11x10^{-6}$ M)	6063Al-Si alloy	$0.5MH_3PO_4$	72.5	41
Clotrimazole(CTM) ($1x10^{-4}$M) Fluconazole (FLC) ($1x10^{-4}$M)	Al	0.1MHCl	88.0 82.0	42
Fluconazole ($8x10^{-5}$ M)	Al	0.1MHCl	76.5	43
Meclizine hydrochloride (500ppm)	Al	1MHCl	92.9	44
Metronidazole(300ppm)	6061Al-Si alloy	0.1MHCl	95.5	present work

3.12. (FT – IR)analysis

The FT-IR spectrum is a powerful tool which used to investigate the compound functional groups and their interactions with the metal surface. Since organic compounds such as drugs are absorbed on the metal surface which improves resistance against corrosion, and FT-IR can be used to analyze the surface changes to prove the nature of the chemical components which adsorbed on the surface[45].

The FTIR spectrum of pure MNZ is shown in Figure 14 [46]. The FTIR spectrum of the passive film is shown in Figure 14. It is found that the intra molecular hydrogen bonding of O-H stretching has shifted from 3218.37 cm⁻¹ to 3216.44 cm⁻¹. The C-NO₂ stretching has shifted from 1533.47 cm⁻¹ to 1531.52 cm⁻¹. The C = N stretching frequency shifts from 1654.25 cm⁻¹ to 1651.14 cm⁻¹. These shifts approve the presence of adsorbed MNZ film on the surface.
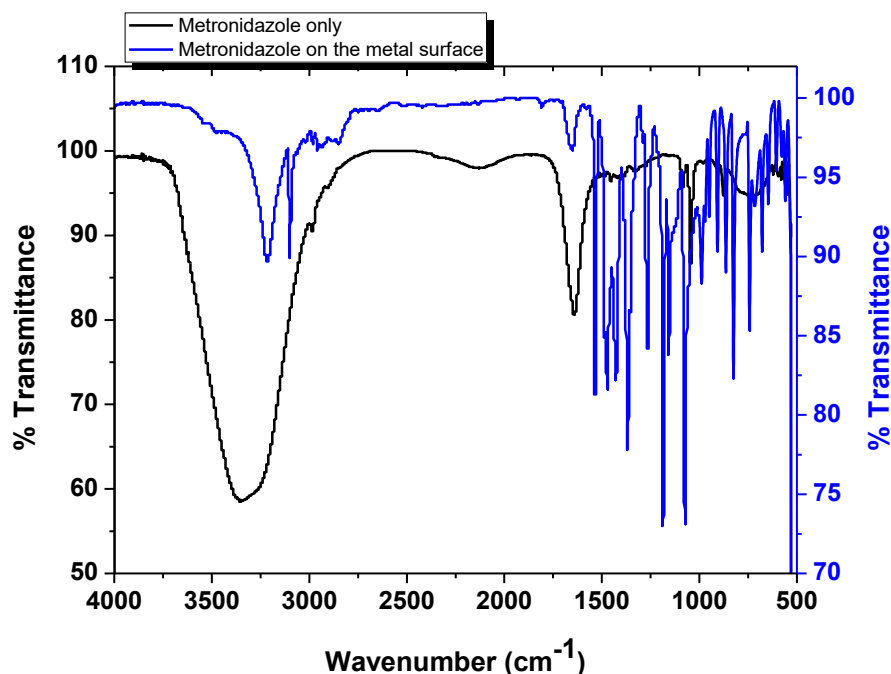
Figure 14. FT-IR spectra of Metronidazole solution (1000 ppm) (black spectrum line) and protective film of Metronidazole on Al alloy surface (the blue spectrum line)

4. CONCLUSIONS

The MNZ shows the corrosion inhibition for Al alloy in HCl solution, where IE ratio improved by rise of compound concentration. The IE is decreasing with rise of temperature resulting from the destruction of the adsorbed MNZ molecules present on the Al alloy surface. The presence of Metronidazole on the surface follows Temkin equation. Tafel curves showed that MNZ is mixed-kind inhibitors. (C_{dl}) reduced by the rise of the MNZ concentration. While (R_{ct}) rise. The adsorbed passive layer on the Al alloy surface was proved by AFM, SEM and FTIR analyses.

References

1. N. Hajjaji; I. Ricco, A. Srhiri, A. Lattes, M. Soufiaoui and A. Benbachir, *Corrosion*, 49(1993)326
2. M. Elachouri, M.S. Hajji, M. Salem, S. Kertit, R. Coudert and E.M. Essassi, *Corros.Sci.*, 37(1995) 381
3. H. Luo, Y.C. Guan and K.N. Han, *Corrosion*, 54(1998)619
4. M.A. Migahed, E M S. Azzam and A.M. Al-Sabagh, *Mater.Chem.Phys.*, 85(2004) 273
5. M.M. Osman, A.M.Omar and A.M. Al-Sabagh, *Mater.Chem.Phys.*, 50 (1997) 271
6. F. Zucchi, G. Trabanelli and G. Brunoro, *Corros.Sci.*, 33 (1992) 1135
7. R.F.V. Villamil, P. Corio, J.C. Rubim and M.L. Siliva Agostinho, *J. Electroanal.Chem.*, 472 (1999)112
8. T.P. Zhao and G.N. Mu, *Corros.Sci.*, 41(1999)1937
9. S.S. Abd El Rehim, H. Hassan and M A. Amin, *Mater.Chem.Phys.*, 70 (2001) 64
10. S.S. Abd El Rehim, H. Hassan., M and A. Amin, *Mater.Chem.Phys.*, 78(2003)337
11. R. Guo T. Liu and X. Wei, *Colloids Surf.*, A, 209(2002)37

12. V. Branzoi, F. Golgovici, F. Branzoi, *Mater.Chem.Phys*., 78(2002)122
13. Adriana Samide,Petru Ilea and Ana-Cristina Vladu, *Int. J. Electrochem. Sci*.,12(2017)5964
14. H .Ma, S.Chen, L .Niu, S. Zhao, S. Li, and D. Li, *J. Appl. Electrochem*., 32(2002) 65.
15. R. W. Bosch, J. Hubrecht, W. F. Bogaerts, and B. C. Syrett, *Corrosion*, 57(2001)60.
16. S. S. Abdel–Rehim, K. F. Khaled and N. S. Abd–Elshafi, *Electrochim. Acta* 51 (2006) 3269.
17. A. S. Fouda, A. Abdel Nazeer and W. T. El behairy, *Journal of Bio- and Tribo-Corrosion* (2018) 4:7
18. M. El Achouri, S. Kertit, H.M. Gouttaya, B. Nciri,Y. Bensouda, L. Pere, M. RInfante and K. Elkacemi, *Prog. Org. Coat*., 43(2001) 267.
19. S. F. Mertens, C. Xhoffer, B. C. Decooman and E. Temmerman, *Corrosion*, 53 (1997) 381.
20. M. Lagrenée, B. Mernari, M. Bouanis, M. Traisnel and F. Bentiss, *Corros. Sci*., 44 (2002) 573.
21. F. Bentiss, M. Lagrenée, and M. Traisnel, *Corrosion*, 56 (2000)733.
22. E. Kus and F. Mansfeld, *Corros. Sci*.,48 (2006) 965.
23. D. Q. Zhang, Q. R. Cai, X. M. He, L. X. Gao, and G. S. Kim, *Mater. Chem. Phys*., 114(2009) 612.
24. 30. G. Trabanelli, in "Corrosion Mechanisms" (Ed. F. Mansfeld) Marcel Dekker, New York, (1987)119.
25. A.S. Fouda, A. Abd El-Aal and A.B. Kandil, *Desalination*, 201 (2006) 216.
26. A. Fiala, A. Chibani, A. Darchen, A. Boulkamh and K. Djebbar, *Appl. Surf. Sci*., 253(2007)9347.
27. W. Durnie, R.D. Marco, A. Jefferson and B. Kinsella, *J. Electrochem. Soc*., 146(1999) 1751.
28. M. K. Gomma and M. H. Wahdan; *Mater. Chem. Phys*. 39 (1995) 209.
29. A. N. Frumkin, Hydrogen overvoltage and adsorption phenomena. In: Delahay P, Tobias CW (eds) Advances in electrochemistry and electrochemical engineering, vol 3, chapter 5. Interscience Publisher Inc., New York, (1963)].
30. F. Bensajjay, S. Alehyen, M. El Achouri and S. Kertit, *Anti-Corros. Meth. Mater*. 50 (2003) 402
31. L.Tang, X.Li, Y.Si, G.Mu and G.Liu, Mater. Chem. Phys., 95 (2006) 29.
32. G.Mu, X. Li and G.Liu, Corros. Sci., 47 (2005) 1932.
33. B. Wang, M. Du, J. Zang and C.J, Gao, *Corros.Sci*., 53 (2011) 353.
34. S. Rajendran, C. Thangavelu and G. Annamalai, *J.Chem. Pharm.l Res*., 4 (2012) 4836
35. A.S. Fouda, Y.M. Abdallah and D. Nabil, *IJIRSET* 3(2014)12965
36. M. Abdallah, I. Zaafarany, S.O. Al-Karanee and A.A. Abd El-Fattah , *Arabian Journal of Chemistry,* 5(2012) 225
37. R. S. Abdel Hameed, E. A. Ismail, A. H. Abu- Nawwas and I. H. AL-Shafey*, Int. J. Electrochem. Sci.,* 10 (2015) 2098
38. M. Abdallah, *Corros. Sci*. ,46 (2004) 1981
39. O. Paul Ameh and M. Umar Sani, *Journal of Heterocyclics* , 1(1)(2015) 1
40. M.N. Ismail, H.E.Megahed, A. I.Ali and M. A. El-Etre, *Egypt. J. Chem. ,*60(1) (2017)95
41. A.S. Fouda , A.A. Al-Sarawy , F.Sh. Ahmed and H.M. El-Abbasy ,*Corros. Sci*., 51 (2009) 485
42. I.B. Obot , N.O. Obi-Egbedi and S.A. Umoren , *Corros. Sci*., 51 (2009) 1868
43. I. B. Obot , N. O. Obi-Egbedi , S. A. Umoren and E. E. Ebenso , *Chem. Eng. Comm.*, 198 (2011)711
44. J. Ishwara Bhat , V. D. P. Alva, *Trans Indian Inst Met,* 64(4–5) (2011)377
45. W. Chen, S. Hong, H. B. Li, H. Q. luo, M. Li and N. B. Li; *Corros. Sci*. ,61 (2012)53
46. S.M. Megalai,P. Manjula,K.N. Manonmani,N. Kavitha and N. Baby, *Portugaliae Electrochimica Acta*, 30(6), (2012)395